Validating the acceptance zone for PV modules using a simplified measuring approach

Arthur James Swart
Central University of Technology
Department of Electrical, Electronic and Computer Engineering
Bloemfontein, South Africa
drjamesswart@gmail.com

Pierre Eduard Hertzog
Country Central University of Technology
Department of Electrical, Electronic and Computer Engineering
Bloemfontein, South Africa

***Abstract*—Optimizing the output power of any PV module involves a number of factors, including the tilt angle, orientation angle and environmental conditions. However, many PV modules are not installed at the suggested orientation angle of 0° N in South Africa, thereby indicating a non-alignment to the maximum solar radiation available for a given day. The purpose of this research is to highlight the importance of this installation by validating its acceptance zone using a simplified measuring approach. Results confirm that the incident angle on a specific PV module installation varies around 44° for winter months. This indicates an acceptance zone of around 88°, which must be optimally aligned to the solar radiation curve, thereby yielding the optimum amount of output power for a given location.**

***Keywords*–Alignment; Azimuth angle; flat surface; incident angle; tilted surface**

I. INTRODUCTION

Optimizing the output power of any PV module involves a number of factors, including the tilt angle, orientation angle and environmental conditions [1, 2]. Research has shown that PV modules should be installed at an orientation angle of 0º N or 0º S, depending on whether the installation site is in the Southern or Northern hemisphere [3]. This will enable the PV module to be aligned to the largest portion of the solar radiation curve which peaks during midday (12:00 noon), which may be equated to the common bell-shaped curve [4]. At this point in time, the direct beam solar radiation has the smallest Zenith angle to the PV module. However, when considering numerous PV installations in both hemispheres, it is found that their orientation angle is not always set to 0º N or 0º S. This indicates that the maximum solar radiation is not always being optimally received by the PV module, which generally has an efficiency of less than 20%.

Figure 1 highlights the installation of two different PV arrays in Brighton, UK. They are set to the same tilt angle, but not to the same orientation angle. The tilt angle is defined as the angle between the PV module surface and the horizontal plane [5]. The orientation angle is defined as the angle between true South (or true North) and the projection of the normal of the PV module to the horizontal plane [6]. Although it may not be practical to orientate all these roof-installation PV arrays to 0° N or 0° S, it does impact on the conversion efficiency.

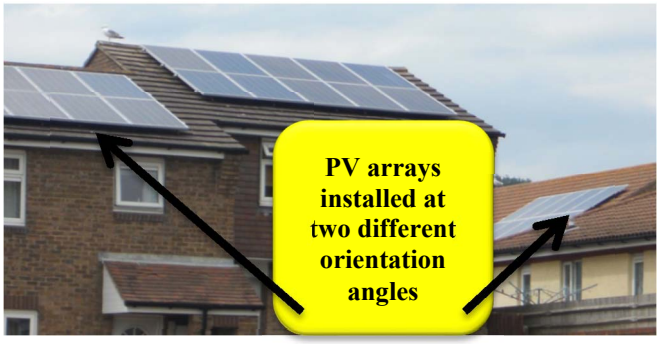

Fig. 1. PV arrays at different orientation angles in Brighton, UK – photo taken during July 2015 by the researcher

Conversion efficiency is defined, in this article, as the percentage of time in which a PV module is producing at least 15% of its peak output power within any given day. The 15% value is derived from research done by Swart and Hertzog [7] and is related to at least 50% of the PV modules maximum power point voltage and 33% of its maximum power point current. A higher percentage of time equates to higher power efficiency and to a larger overall output power for that given day. It must be noted that PV modules generally have low efficiencies, and must therefore be aligned to as much of the direct beam solar radiation as possible to generate the optimum amount of output power for a given day.

The purpose of this paper is to present empirical evidence validating the acceptance zone of a PV module, which must be aligned to the solar radiation curve for a given location, installed in a semi-arid region using a simplified measuring approach. The target area of this research is located in the heart of South Africa (Bloemfontein, Free State) in the Southern Hemisphere which has very little rainfall between May and July, thereby enabling multiple measurements to be obtained

978-1-4673-9749-0/16/$31.00 ©2016 IEEE

with no severe cloud interference. The relationship between incident angles of optic fiber cables, acceptance angles of concentrated PV systems, radio-frequency (RF) antenna beam widths and the acceptance angle of a PV module will firstly be given. The practical setup and methodology will then be substantiated. Descriptive results, in the form of sketches and tables, will be presented, along with succinct conclusions.

II. Relationships and Equations for Angles

The angle between the direct beam solar radiation and the normal of a PV modules' surface may be termed the incident angle. This incident angle may be correlated to the angle of incidence of an optic fibre cable, to the acceptance angle of a concentrated solar power system or to the -3 dB beam width of a RF antenna. In the case of an optic fibre cable, the angle of incidence (see Figure 2 for its position) needs to be larger than the critical angle so as to ensure total internal reflection [8]. This critical angle is defined by the refractive indexes of the core and cladding material.

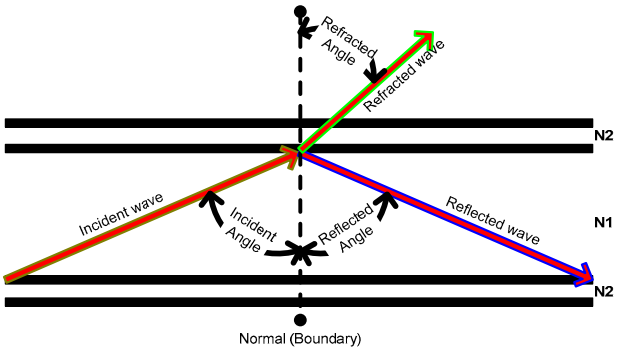

Fig. 2: Angles within an optic fibre cable measured from the normal

In the concentrated solar power field, the acceptance angle is defined as the misalignment angle of the sunlight at which point it still delivers at least 90% of its maximum power [9]. This acceptance angle is defined as twice the incident angle (position shown in Figure 3), and is referred to in this paper as the acceptance zone of a PV module.

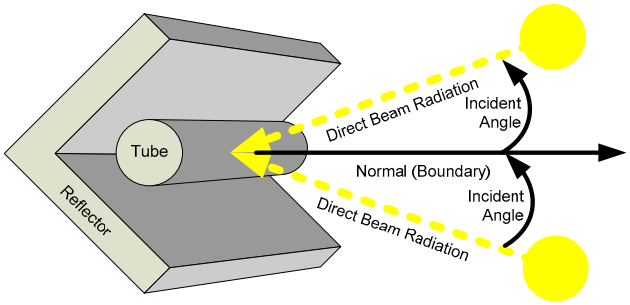

Fig. 3: Incident angle of a concentrated solar power system

In the case of a RF antenna's beam width, specific electromagnetic waves need to be received within the beam width (see Figure 4 for its position) to enable an acceptable level of system performance [10]. This beam width is usually defined by the type of antenna design, where the inclusion of more directors will result in a smaller beam width. Similarly, the direct beam solar radiation needs to fall within a given acceptance zone (being twice the defined incident angle) to ensure that the PV module's surface is exposed to the major portion of the solar radiation curve available for any given day.

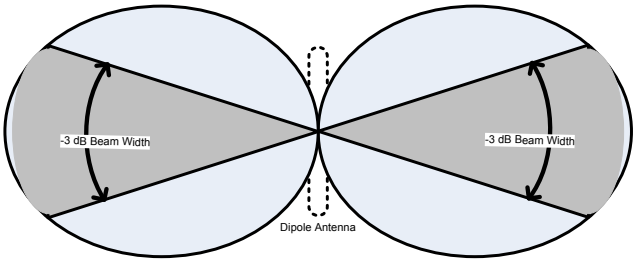

Fig. 4: Radiation pattern of a vertically polarized Dipole antenna

The previous three figures highlight that these different systems (optic fibre, concentrated PV and RF antennas) have the same generic parameter, that of receiving specific energy within a given angle or zone to ensure optimum performance. This generic parameter may also be applied to PV modules, which need to be aligned to the major portion of the solar radiation curve for a given day to enable optimum output power. Figure 5 highlights the position of the tilt angle, where 3 identical PV modules have been set to different values corresponding to research done by Heywood [11] and Chinnery [12]. Figure 5 further shows the Zenith angle which indicates the constantly changing angle between the path of the sun through the sky and the Zenith (straight line through the centre of the earth but perpendicular to the surface).

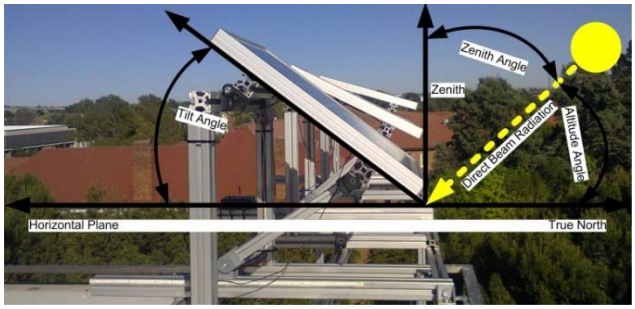

Fig. 5: Different tilt angles visible on this PV array

The different tilt angles correspond to Latitude, Latitude + 10° and Latitude – 10°. A tilt angle of 29° was used in this research which corresponds to the Latitude value of the installation site at the Central University of Technology (CUT). This tilt angle significantly influences the defined incident angle as shown in the following equations taken from previous research in this field [13, 14]:

$$\theta_{i\_tilt} = \cos^{-1}[A - B + C + D + E] \quad (1)$$

$$A = \sin(\phi) \times \sin(\delta) \times \cos(\beta) \quad (2)$$

$$B = \cos(\phi)\times\sin(\delta)\times\sin(\beta)\times\cos(\gamma) \quad (3)$$

$$C = \cos(\phi)\times\cos(\delta)\times\cos(\beta)\times\cos(\omega) \quad (4)$$

$$D = \sin(\phi)\times\cos(\delta)\times\sin(\beta)\times\cos(\gamma)\times\cos(\omega) \quad (5)$$

$$E = \cos(\delta)\times\sin(\beta)\times\sin(\gamma)\times\sin(\omega) \quad (6)$$

Where

ϕ $\equiv Site\ Latitude\ (Radians)$

δ $\equiv Site\ Declination\ Angle\ (Radians)$

β $\equiv PV\ Tilt\ Angle\ (Radians)$

γ $\equiv PV\ Orientation\ Angle\ (Radians)$

ω $\equiv Hour\ Angle\ of\ the\ sun\ (Radians)$

n $\equiv Day\ number\ of\ the\ current\ year$

Equations 2 through 6 must first be used in determining the incident angle between the direct beam solar radiation and the PV modules tilted surface. A key parameter in these equations is the tilt angle (β) of the PV module, which is fixed at 29° for this research, corresponding to the fixed Latitude value of the installation site. However, changing this tilt angle value will result in a corresponding change in the incident angle for a given day. The hour angle of the sun changes constantly through the day, while the site declination will change every day, being calculated using equation 7 [15]. The orientation angle of the PV module is fixed at 0° N (see Figure 6 for its position) while the hour angle of the sun is calculated using equation 8 (adapted from research done by Ng et al. [16] and by Castenmiller [17]).

$$\delta = 23.45\times\frac{\pi}{180}\times\sin\left[2\times\pi\times\left[\frac{284+n}{365.25}\right]\right] \quad (7)$$

$$\omega = [12-[Site\ Hour + \frac{Site\ Minutes}{60}]]\times 15 \quad (8)$$

The day number of the year may be calculated using equation 9 (for the first two months of the year) or equation 10 (for March through December).

$$n = floor[(\frac{Month-1}{12}\times 372) + Date] \quad (9)$$

$$n = floor[(\frac{Month-1}{12})\times 366 + (Date - 1.5)] \quad (10)$$

Three of the parameters used in calculating the incident angle on a tilted surface may also be used to calculate the incident angle on a flat surface, as shown in equation 11. The site latitude, declination angle and hour angle are required for this equation adapted from Castenmiller [17].

$$\theta_{i\_flat} = \cos^{-1}[\cos(\phi)\times\cos(\delta)\times\cos(\omega) + \sin(\phi)\times\sin(\delta)] \quad (11)$$

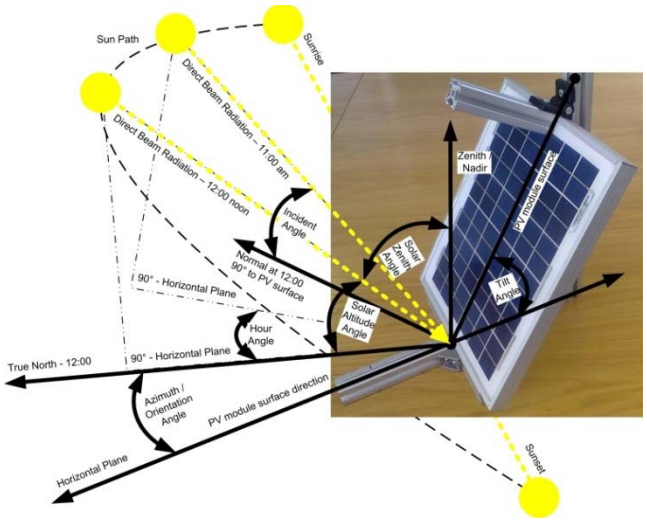

Fig. 6: PV module geometry showing different angles

Results of equation 11 may be correlated to the degrees of a physical protractor placed perpendicularly on a flat surface where a wooden dowel from the protractor's center is manually aligned to the suns' rays (see Figure 7). Aligning the dowel with the direct beam solar radiation so that no shadow is cast on either side of the dowel will provide a visual indication to an observer of the given incident angle.

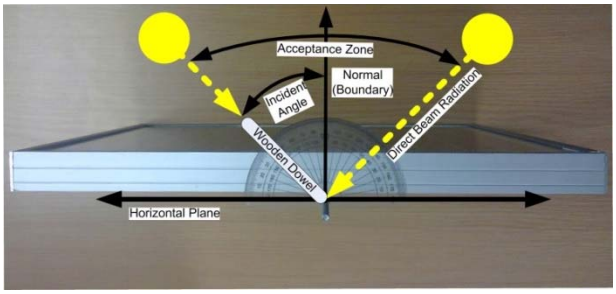

Fig. 7: Incident angle from a protractor on a PV module

The normal (or boundary) coincides with the 90° line of the protractor, and presents the optimum incident angle of 0° for maximum output power from a PV module. The acceptance zone is visible in being twice the defined incident angle for a given PV installation. It must be re-iterated that the defined incident angle must enable the PV module to start producing at least 15% of its peak output power. This 15% value is derived from research done by Swart and Hertzog [7] which indicates that the PV module is receiving direct beam solar radiation, rather than only diffused or reflected radiation which is not conducive to optimal PV system performance.

Constantly aligning a wooden dowel to the incoming direct beam solar radiation to ascertain its incident angle on a flat surface proves tedious and time consuming. Furthermore, parallax errors may be made by the observer. Another option is to place the protractor parallel to the flat surface and make use of a gnomon (Greek word meaning "one that knows or examines"). A gnomon is a perpendicular pin or dowel placed at the centre of the protractor that causes a shadow to fall over the angles of the protractor which correspond to the hour angle of the sun as it moves across the sky. It is typically used in sundials to indicate the time of day (see Figure 8) where the horizontal plane must coincide with the equatorial plane. A more accurate method of calculating the hour angle would involve using the so called equation of time [18]. The gnomon method does not accurately indicate the incident angle of the sun's rays on a flat surface. However, it does serve as a general indication of the size of the incident angle when considering Figure 6. A larger hour angle value will indicate a larger incident angle value when the PV module is orientated to 0° N or S, and vice versa. The main advantage of this method is that no manual alignment of any dowels is required, enabling a camera to be focused on it to take snapshots for predefined moments at any time of the day.

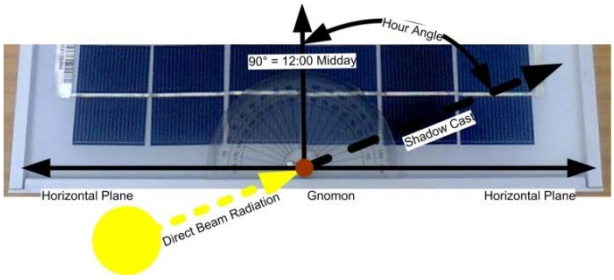

Fig. 8: Hour angle from a protractor on a PV module

The time of sunrise and the number of day hours available for a given date may furthermore be calculated using equations 12 and 13 [16]. These equations may be used to verify the accuracy of the calculated declination angle as it is accepted that the number of day hours is less in winter than in summer. Severe winter months in South Africa include June and July, which is the time period when the simplified measuring approach was used to validate the acceptance zone.

$$\omega_{Sunrise} = \cos^{-1}[\tan(\phi)\times\tan(\delta)] \quad (12)$$

$$Day_{Hours} = \frac{2\times\omega_{Sunrise}}{15}\times\frac{180}{\pi} \quad (13)$$

III. Practical Setup of the Simplified Approach

The simplified measuring approach (see Figure 9 for the setup) consists of a 10 W peak polycrystalline PV module, a 60 LED Lamp (MR16, rated 3 W at 12 V), a protractor, a Webcam (Prestigio), an aluminum frame, a notebook and a software package for motion detection (Yawcam). A number of research articles have been published where LED lamps were used as load resistances for PV modules [7, 19]. The majority of LED Lamps do not have a threshold voltage which can be adjusted by means of a series resistor. However, this specific 60 LED Lamp has a unique driver circuit which may be manipulated by using a series resistor to adjust the threshold operating voltage, thereby ensuring that a higher output power would be required from the PV module to activate it [7]. This series resistor also ensures that the voltage over the 60 LED Lamp never exceeds 13 V, as the maximum power point voltage from the PV module is 16.5 V. A 22 Ω resistor was therefore used based on previous research [7]. It must be noted that 3 W is the maximum power rating of the LED, which does activate at lower power values.

An aluminum frame was constructed to securely mount the 10 W PV module at a tilt angle of 29º, equating to the latitude value of 29º for CUT [20, 21]. CUT is located in the semi-arid part of South Africa that enjoys 55% of its annual rainfall between January and April [22], with very little rainfall during the winter months of May through August. The practical setup was done inside an air-conditioned room where the temperature was kept constant at 25^{0}C. This was in order to prevent excess temperature degradation which has a significant effect on the output voltage of a PV module [23].

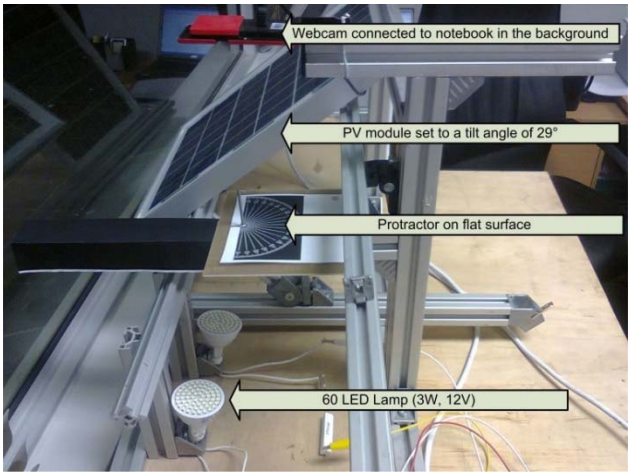

Fig. 9: Practical setup showing the various components

The Webcam was focused on the 60 LED Lamp and protractor, in order to take a snapshot when signaled by the motion detection option available in the software package when the LED is activated. The sensitivity of the motion detection was set to 75% with a tolerance value of 15%. A higher tolerance value implies that a significant amount of motion needs to occur for the Webcam to be signaled. Multiple snapshots were taken over a 3 month period where the timestamp and protractor value where visually observed and recorded in an Excel sheet (part of the methodology).

IV. Methodology

An experimental research design is used to gather quantitative data from snapshots taken from a Webcam (data

collection instrument). The timestamp was obtained from the file name and the value of the hour angle on a horizontal surface was visually determined from the shadow cast on the protractor in the snapshot (see Figure 10).

This data was recorded in an Excel sheet, where equations 1 through 11 where used to calculate the incident angle on a tilted and horizontal surface. Correlations were made between the hour angle derived from the protractor and the calculated tilt values. Data was recorded from May to July of 2015 which corresponds to the winter months for the installation site. The setup was installed in an office with a north facing window to ensure that the ambient temperature never exceeded 25ºC. Motion detection was limited to a specific area defined in the software package in order to avoid numerous snapshots of unrelated or erroneous events. This area was defined to include only the 60 LED Lamp, and not the rest of the practical setup. The analyzed results from the Excel sheet are presented next in a series of graphs and tables.

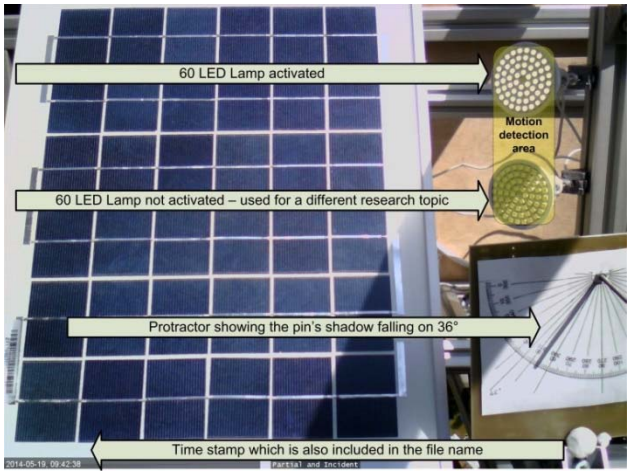

Fig. 10: Example of a snapshot taken on the 19 May 2015

V. RESULTS

Figure 11 shows the results of using equations 1 through 6 where two specific variables were entered into Excel, namely the timestamp at which the LED was activated and the date on which it occurred. The day of the year (using equation 10), the declination angle (using equation 7) and the hour angle (using equation 8) where calculated automatically in Excel using the two specific variables. Results indicate that the incident angle varies between 41° and 46° for the period of interest when the PV module is required to produce at least 15% of its peak output power. The most common incident angle was 44° which had a combined frequency count of 16.

Table I present's descriptive statistics of the calculated values for the incident angle upon a tilted surface (equations 1 through 6) and a flat surface (equation 11). The time period is shown to be from 19 May to 9 July 2015, featuring 37 samples in total. Cloudy conditions (insufficient direct beam solar radiation) or computer operating system concerns (MS Windows freezing) resulted in a number of days being lost. Figure 12 graphically portrays the actual values recorded over the time period of interest.

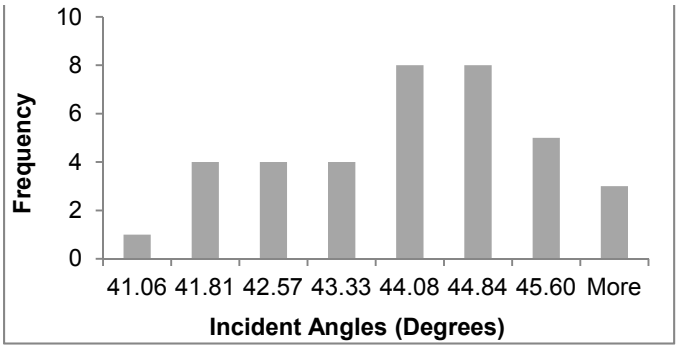

Fig. 11: Incident angle frequency counts on a tilted surface

TABLE I: Descriptive statistics of the calculated values for the incident angle

Descriptive statistics of the inclination angle for a:		
Parameters:	Tilted surface	Flat surface
Time period	19 May 2015 – 09 July 2015	
Mean	43.73	31.32
Median	43.81	31.81
Standard Deviation	1.41	2.72
Kurtosis	-0.73	-0.35
Skewness	-0.21	-0.71
Minimum	41.06	25.48
Maximum	46.35	35.25
% error to the protractor	NA	8.80%
Count	37.00	37.00
Pearson correlation	0.92	0.98
Significance	13.78	27.28
p-value	0.000	0.000

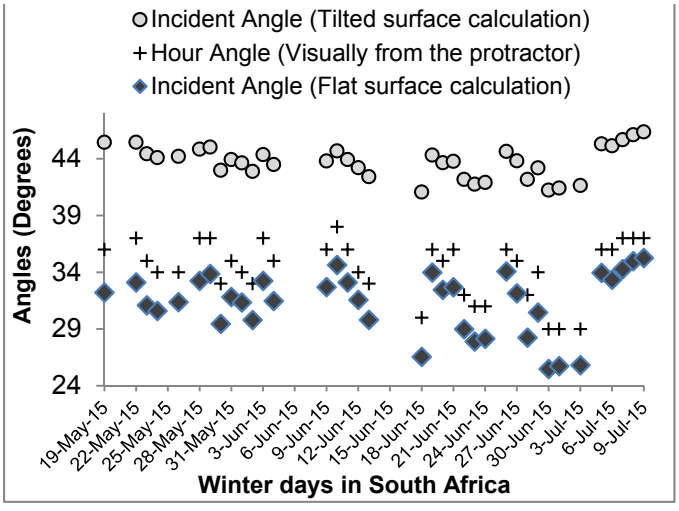

Fig. 12: Incident angle (calculated) compared to the hour angle (protractor)

The data shown in Table I does indicate that the standard deviation is less than 1.41 (3.2% from the mean) for the tilted

surface and 2.72 (8.7% from the mean) for the flat surface. These low standard deviations indicate a high consistency of the results which indicates validity and reliability of the simplified measuring approach. Noteworthy too is the average percentage difference between the visually observed protractor values (hour angle) and the calculated values for a flat surface (only 8.8%). A Pearson correlation indicates a statistically significant relationship between the calculated values and that obtained visually from the protractor, thereby validating it as a general indication of the incident angle.

VI. CONCLUSIONS

It has been stated that energy losses are associated with incident angles larger than 45° in PV modules [3]. The optical efficiency of specific PV concentrators has also been found to drop of significantly with incident angles larger than 55° [24]. This indicates that as the sun moves across the sky from east to west, the incident angle varies drastically, resulting in a subsequent decrease of direct beam solar radiation falling in on the PV module, as more of the energy reflects off the glass rather than being absorbed. In this research, it was found that a PV module (tilt angle of 29° and an orientation angle of 0° N or S) produces 15% of its peak output power when the incident angle was between 41° and 46° for specific days during winter months in South Africa. Previous research, mentioned at the outset of the conclusion, corroborates these findings; thereby validating the use of this simplified measuring approach requiring a 60 LED Lamp, Webcam and motion detection software. The reason for using a LED lamp is to be able to visually observe the switch-on time of the PV module, in able to correlate it to the hour angle of the sun and its subsequent incident angle on the inclined PV module. This enables multiple automatic snapshots to be acquired when the LED is activated, thereby providing the exact time of day when the PV module starts producing at least 15% of its peak output power. Using this exact time with predefined equations from previous research yields the acceptance zone of 82° to 92° for a PV module installed in a semi-arid region of South Africa. This acceptance zone must be aligned to the solar radiation curve, which usually follows a bell shaped curve, in order to yield the optimum amount of output power.

ACKNOWLEDGMENT

This work is based on the research supported in part by the National Research Foundation (NRF) of South Africa. Any opinions, findings, conclusions or recommendations expressed in this material are that of the author(s) and the NRF does not accept any liability in this regard.

REFERENCES

[1] O. Asowata, *et al.*, "Optimum Tilt Angles for Photovoltaic Panels during Winter Months in the Vaal Triangle, South Africa," *SGRE, Smart Grid and Renewable Energy,* vol. 3, pp. 119-125, 2012.

[2] A. J. Swart, *et al.*, "Assessing the effect of variable atmospheric conditions on the performance of photovoltaic panels: A case study from the Vaal Triangle," presented at the Southern African Energy Efficiency Convention, SAEEC 2011, Emperor's Palace Convention Centre, Johannesburg, 2011.

[3] O. Asowata, *et al.*, "Evaluating the effect of orientation angles on the output power of a stationary photovoltaic panel," *JRSE, Journal of Renewable and Sustainable Energy,* vol. 6, pp. 1-9, 2014.

[4] Y. Su, *et al.*, "Real-time prediction models for output power and efficiency of grid-connected solar photovoltaic systems," *Applied Energy,* vol. 93, pp. 319-326, 2012.

[5] S. Pradabane, *et al.*, "A New Alternate Fixed-Bias Inverter SVPWM Scheme for Open-End Winding Induction Motor Drive," *International Review of Electrical Engineering (IREE),* vol. 9, pp. 1-6, 2014.

[6] C. Hachem, *et al.*, "Design of roofs for increased solar potential BIPV/T systems and their applications to housing units," *ASHRAE Transactions,* vol. 118, p. 660, 2012.

[7] A. J. Swart and P. E. Hertzog, "Quantifying the Effect of Varying Percentages of Full Uniform Shading on the Output Power of a PV Module in a Controlled Environment," presented at the SATNAC 2014, Boardwalk Conference Centre, PE, South Africa, 2014.

[8] B. Y. Zeldovich and C. Tsai, "An electromagnetic world without polarization," *Journal of Optics,* vol. 15, p. 014014, 2013.

[9] Y.-P. Huang and P.-F. Tsai, "Improving the Output Power Stability of a High Concentration Photovoltaic System with Supercapacitors: A Preliminary Evaluation," *Mathematical Problems in Engineering,* vol. 501, p. 127949, 2015.

[10] C. Maccone, "So much gain at 550 AU," in *Mathematical SETI*, ed: Springer, 2012, pp. 335-347.

[11] H. Heywood, "Operating experiences with solar water heating," *Journal of Installation Heat Venting Energy,* vol. 39, pp. 63-69, 1971.

[12] D. N. W. Chinnery, "Solar heating in South Africa," Pretoria CSIR-Research Report 248, 1981.

[13] S. A. Klein, "Calculation of monthly average insolation on tilted surfaces," *Solar Energy,* vol. 19, pp. 325-329, 1977/01/01 1977.

[14] J. A. Duffie and W. A. Beckman, "Solar Thermal Power Systems," *Solar Engineering of Thermal Processes, Fourth Edition,* pp. 621-634, 2014.

[15] P. Cooper, "The absorption of radiation in solar stills," *Solar Energy,* vol. 12, pp. 333-346, 1969.

[16] K. M. Ng, *et al.*, "Assessment of solar radiation on diversely oriented surfaces and optimum tilts for solar absorbers in Malaysian tropical latitude," *International Journal of Energy and Environmental Engineering,* vol. 5, pp. 1-13, 2014.

[17] C. Castenmiller, "Surface temperature of wooden window frames under influence of solar radiation," *Heron,* vol. 49, pp. 339-348, 2004.

[18] T. D. Liebermann, "Calculation of the daily and instantaneous potential solar radiation and solar angles on sloping surfaces," in *Proc. of the 11. annual ESRI user conference*, 1990.

[19] T. Anandhi and S. PremKumar, "Application of DC-DC Boost Converter for Solar Powered Traffic Light with Battery Backup," *Indian Journal of Science and Technology,* vol. 8, 2015.

[20] P. E. Hertzog and A. J. Swart, "Determining the optimum tilt angles for PV modules in a semi-arid region of South Africa for the summer season," presented at the SATNAC 2015, Arabella, Hermanus, Western Cape, 2015.

[21] P. E. Hertzog and A. J. Swart, "The Use of An Innovative Jig to Stimulate Awareness of Sustainable Technologies among Freshman Engineering Students," *Sustainability,* vol. 7, pp. 9100-9117, 2015.

[22] H. Snyman, *et al.*, "Ranking of grass species according to visible wilting order and rate of recovery in the Central Orange Free State," *Journal of the Grassland Society of Southern Africa,* vol. 4, pp. 78-81, 1987.

[23] A. Ozemoya, *et al.*, "Poster: Controlling the ambient temperature of a PV panel to maintain high conversion efficiency," in *SATNAC 2012*, George, South Africa, 2012.

[24] N. Sarmah, *et al.*, "Evaluation and optimization of the optical performance of low-concentrating dielectric compound parabolic concentrator using ray-tracing methods," *Applied Optics,* vol. 50, pp. 3303-3310, 2011/07/01 2011.